Journal of Applied Sciences

ISSN 1812-5654

science alert

ANSInet
an open access publisher
http://ansinet.com

Journal of Applied Sciences 8 (17): 3012-3018, 2008
ISSN 1812-5654

Influence of Peaks Raindrop Size Distribution on the Variability of the Reflectivity Radar

[1]M. Koffi, [1]Z. Yeo, [1]A. Tanoh, [2]A.D. Ochou, [1]O. Asseu, [1]D.K. Konan and [1]M.A. Kouacou
[1]Department of Electrical and Electronic Engineering,
Institut National Polythechnique Houphouet Boigny, (INP HB) BP 1093, Yamoussoukro, Côte d'Ivoire
[2]Université de Cocody, Abidjan Côte d'Ivoire

Abstract: The raindrop size distribution (DSD) measurements were collected in the tropical and mid-latitude rain system. Comparisons of measured values and estimated values of polarimetric parameters (Z_H and Z_{DR}) shows that kinematic peaks are the main cause of the variability of Z_H but they do not influence much Z_{DR}. The influence of the peak number on the variance of the radar parameters is based on the relations between time and averaging. It consists to examine how many DSDs have to be averaged in order to suppress the peaks and what are the consequences on the radar parameters. The study shows that averaging improves the validity of the polarimetric parameters.

Key words: Peaks, rain drop distributions, reflectivity factor at orthogonal, differential reflectivity factor, variance and radar

INTRODUCTION

The raindrop size distributions (DSDs) characteristics depend on the microphysical, dynamical and kinetic processes that interact to product rain. They are the basis for the definition and computation of the major part of parameters involved microware propagation within clouds and rain. Radar reflectivity factor and electromagnetic attenuation depend on the DSD (Coppens and Haddad, 2000; Iguchi *et al*., 2000), that is why, appreciable effort has been made for observing, understanding and modeling the DSDs (Maki *et al*., 2001; Atlas and Ulbrich, 2000; Testud *et al*., 2001; Uijlenhoet *et al*., 2003; Kozu *et al*., 2006; Ochou *et al*., 2007).

Observations and numerical simulations alike suggest that DSDs are not random but reproducible. The shapes of the DSD can be represented with simple functions (exponential, gamma and lognormal). The parameters of these functions depend on the rain type and on the environmental conditions (Sauvageot and Lacaux, 1995; Nzeukou *et al*., 2004). It is admitted that this shape mainly results from coalescence and collisional breakup in such a way that the size of falling raindrops evolves with time toward a distribution independent of the starting conditions but dependent on the number of collision.

It is known that the DSD measured are biased by instrumental artifacts associated with the Joss-Waldvogel disdrometer (Sheppard, 1990; McFarquhar and List, 1993). These artifacts (peaks) are permanent and modify the distribution between some classes. Sauvageot and Koffi (2000) argue that some irregularities observed in the DSD do not seem only attribute to random or instrumental process because of their large amplitude and/or their persistence. These authors attributed the causes of the peaks of some DSDs to an overlapping of precipitation streamers originating from separating cloud volumes located side by side, at the same horizontal level, along a line parallel to the direction of the wind at the generating level. Sauvageot and Koffi (2000) have provided a conceptual model to explain the shapes of resulting from overlapping rain cells. Clearly, the shapes of the distribution display a tendency toward multimodality.

The punctual value of the radar reflectivity factor is determined by the DSD (the space integration associated to the radar pulse volume is similar to the time integration of a DSD at the time step of 1 min). Thus it is useful to better know the variability of the DSD in order to understand and interpret correctly the radar measurement, notably with polarimetric methods (e.g., Ilingworth *et al*., 2002). In this study the direct attention to the sensitivity of the radar parameters to the presence of the peaks. Recent researches indicate that radar reflectivity are less than those of the distrometer (Brandes *et al*., 2002), in this study the discussion relates to the estimated and measured values of polarimetric parameters.

The next object of the study is to analyze the influence of the peaks on the variance of the parameters used for precipitation measurements with radar. This problem is important because using the radar for the

Corresponding Author: Z. Yeo, Department of Electrical and Electronic Engineering,
Institut National Polythechnique Houphouet Boigny, (INP HB) BP 1093, Yamoussoukro, Côte d'Ivoire
Tel: (+00225) 05 01 71 35 Fax: (+00225) 30 64 04 06

observation of the precipitation fields tends to spread; all the industrialized countries obtained dense networks of meteorological radars for precipitation measurements. West Africa, in the south of the Sahara is equipped with about fifteen radars.

MATERIALS AND METHODS

The sample: The data used in the work was collected at four sites (Fig. 1, Table 1):

- Abidjan is in southern Ivory Coast, on the Guinea Gulf coast, in this area, it is possible to clearly distinguish a long rainy season from March to mid-July, associated with the northward migration of the intertropical convergence zone (ITCZ) and a short rainy season from mid-September to late November, associated with southward migration of the ITCZ. The mean annual total rainfall is about 1800 mm. The region is flat.
- Brest is in Brittany: The mean total rain fall is about 1200 mm. Most of the precipitation is associated with the frontal cyclone systems of the zonal circulation. In winter, these systems are well developed with extended stratiform precipitation.
- Niamey is in southwestern Niger: The rainy season lasts about 3 months, from early July to late September. Niamey is situated in the middle of the Sahelian Sudanese strip. The mean annual total rainfall is about 500 mm. The rainy season is associated with the northward move of the ITCZ. The area is very flat. The most significant rain-generating events are organized in squall lines.
- Boyélé is in the northern Congo: It is located in the upper basin of the Oubangui River in a locally flat region. The mean annual pluviometry is about 1000 mm. The rainy season lasts from early March to late November. The measurement station was situated in the pygmy area, in a vast clearing surrounded by primary equatorial forest. The main precipitating systems are also organized in squall lines.

The data of the two continental Africa Boyélé and Niamey) were gathered in only one sample. They correspond to the same meteorological entity and since the DSD characteristics are essentially identical.

The sensor: DSDs were observed with a Joss and Waldvogel (1969) disdrometer (JWD hereafter). The JWD enables measurements of the size distribution of raindrops by converting the mechanical moments of failing drops into electric pulses. The performances and limitations of this widely used sensor are well known and have been discussed in many papers (e.g., Sauvageot and Lacaux (SL hereafter), 1995; Tokay *et al*., 2001). Only drops with an equivalent spherical diameter D larger than 0.3 are detected. The pulses are transformed in 8 bit numbers and sorted according to 25 size classes, all with a width (ΔD = 0.2 mm), covering diameters ranging between 0.3 and 5.3 mm. The data were systematically corrected for the error due in the dead time of the instrument after the simple area hit by the drops (Sauvageot and Lacaux, 1995). The measuring time span of the DSD is always 1 min.

To study the influence of the peaks, we have to get rid of the instrumental modes of the DSDs. Several methods were tested in order to suppress or filter them from the raw DSDs. However, none proved satisfactory (SK, 2000). Most of the instrumental peaks appear for $D \leq 2$ mm, that is why, the decision was made to eliminate the classes of the DSDs corresponding to $D \leq 2$ mm and work only with $D > 2$ mm (SK, 2000). Doing that, the main mode of the DSDs is also suppressed, since, even in the tropical DSDs where, a deficit in small drops (with respect to the exponential distribution) is observed (e.g., SL,

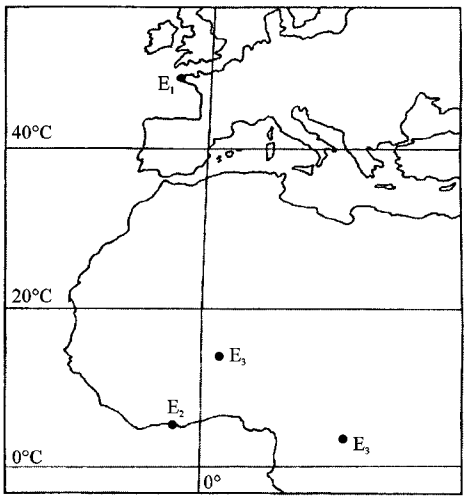

Fig. 1: Location of the data collection sites (Table 1)

Table 1: Data sample designation, here R is rain rate

Location	Brest (France)	Abidjan (Côte d'Ivoire)	Niamey-Boyélé (Niger-Congo)
Designation of the sample	E_1	E_2	E_3
period	Nov. 1987 to Jan. 1996	Nov. 1986 to Dec. 1988	Jun. 1986 to Jul. 1989
No. of 1 min DSD	37184	23389	19713
Rmax (mm h^{-1})	75	130	150

1995), the main mode is usually for D≤2 mm. A low-amplitude mode is also found near 4.0 or 4.2 mm; however, it is not a significant cause of error.

Let, N(D) be the drop size distribution and Z_{Ht}, Z_{hm}, Z_{DRt} and Z_{DRm}, respectively the reflectivity factor at horizontal estimated and measured and the differential reflectivity factor estimated and measured.

Averaged distribution: For this study, three parameter distributions were compared: modified gamma, complete gamma and lognormal. All give acceptable results. The lognormal distribution was chosen because his function provides a good fit to observe DSDs in tropical and continental Africa, the parameters have a simple geometrical interpretation and the moment generating function can be written very simply in the form of a multiplication of three terms.

The log normal distribution has the following expression N(D) is the number density distribution:

$$N(D) = \frac{N_T}{\sqrt{(2\pi)}(\ln\sigma)D}\exp\left[-\ln^2(D/D_g)/2^2\ln\sigma\right]$$

where, N_T is the total number of drops, Dg is the mean geometrical diameter and σ is the standard geometrical deviation of D: namely:

$$N_T = \int_0^\infty N(D)dD,\quad \ln D_g = \overline{\ln D},\quad \ln^2\sigma = \overline{\left(\ln D - \ln D_g\right)^2}$$

Using the data collected in the continental Africa (Niger-Congo), the parameters of the lognormal distribution are given (Sauvageot and Lacaux, 1995):

$$N_T = 86\,R^{0.36}\ (\text{en m}^{-3}) \quad (1)$$

$$D_g = 0.84\,R^{0.23}\ (\text{en mm}) \quad (2)$$

$$\sigma = 1.42 - (3\times10^{-3}\,R)\ (\text{en mm}^{-1}\,\text{m}^{-3}) \quad (3)$$

Radars observables: The two basic radar observables of interest in this work are reflectivity factor at orthogonal (Z_H) and vertical polarizations (Zv), respectively. These are defined by:

$$Z_{H,V} = \frac{\lambda^4}{\pi^5|K|^2}\int_0^{D_{max}}\sigma_{H,V}(D).N(D)dD, \qquad \left(\text{mm}^6.\text{m}^{-3}\right) \quad (4)$$

From witch differential reflectivity Z_{DR} (Seliga and Bringi, 1976) is defined by:

$$Z_{DR} = Z_H/Z_V,\quad Z_{DR}\,(\text{dB}) = 10\log\left(Z_H/Z_V\right) \quad (5)$$

Taking into account the distortion of raindrop:

$$Z_{DR} = 10\log\left[\frac{\sum_0^{D_m} D_e^6 S_H\left(m, a/b\right)N(D_e)}{\sum_0^{D_m} D_e^6 S_V\left(m, a/b\right)N(D_e)}\right]\ [\text{dB}] \quad (6)$$

where, $\sigma_{H,V}(D))$ are the backscattering cross sections for horizontally and vertically polarized microwaves of an oblate raindrop whose volume is equal to that of a corresponding spheroidal raindrop of diameter D (mm), λ(mm) is the radar wavelength, $|K|^2 = 0.93$ is the refractivity factor for liquid water, N (D) is the number of drops per unit volume per unit size interval, the integration is carried out over all diameters $0 < D < D_{max}$ where D_{max} (mm) is the maximum raindrop diameter, m is the refractive index of water and S_H and S_V are the horizontal and vertical shape functions.

RESULTS AND DISCUSSION

Measured values and estimated values of Z_H and Z_{DR}: This study relates to the variations of Z_{Ht}, Z_{Hm}, Z_{DRt} and Z_{DRm} according to R. Z_{Hm} and Z_{DRm} are calculated from the DSD measured by the JWD thus including the peaks. Z_{Ht} and Z_{DRt} are estimated from theoretical DSD calculated with the only value of the rain rate R, with the lognormal distribution (by using [Eq. 1-3] to go from Z to N(D) then [Eq. 6] to obtain estimated Z_{DRt}.

Figure 2 presents the variation of Z_{Hm} according to R for each of the samples E_1 and E_2. The coefficients and the exponents of the relations between the parameters (Z_{Hm} and Z_{Ht}) and R calculated on the samples are indicated in Table 3. They are different for the areas. A good correlation is found between Z_{Hm} and R ($0.97<\rho<0.98$).

In Table 2, it noted that the peaks influence strongly the relation Z_H-R (The coefficients and the exponents of the relations between Z_{Ht} and R are less than those between Z_{Hm} and R); however, it is essentially coefficient A_H which is affected (by a factor 2 for E_1 and E_3). For exponent b_H, the slope of the curves remains between 1.30 and 1.71; this stability of exponent b_H is known (Joss and Waldvogel, 1969).

To test the sensitivity of Z_{DR} to the presence of the peaks, the coefficients and the exponents of the relations between Z_{DRm} and R and those between Z_{DRt} and R are also indicated in Table 2. These coefficients are different from one sample to another. The correlation coefficients are

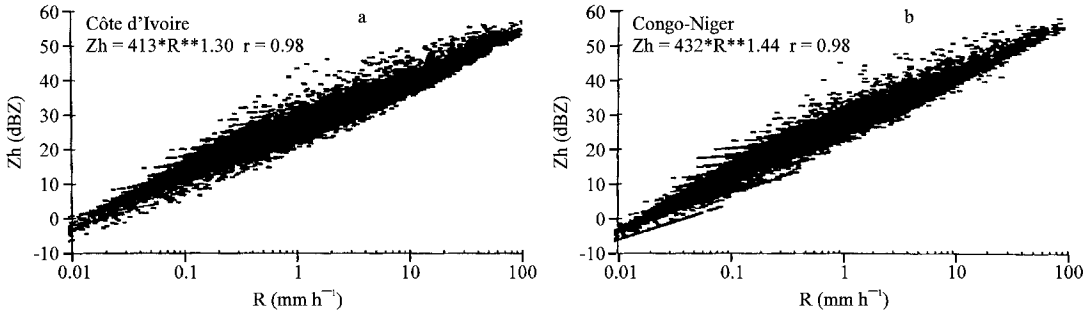

Fig. 2: Variation of Z_{Hm} as a function of R for the sample for the two sites E_2 (a) and E_3 (b)

Table 2: Coefficients of the relations between the radar parameters (Z_{Hm}, Z_{Ht}, Z_{DRm} and Z_{DRt}) and R. ρ is the coefficient of linear correlation. The relations Z_H-R and Z_{DR}-R were obtained by linear regression

	Z_H measured (dBZ) Z_{hm}			Z_H estimated (dBZ) Z_{ht}			Z_{DR} measured (dB) Z_{DRm}			Z_{DR} estimated (dB) Z_{DRt}		
Samples	A_H	b_H	ρ	A_H	b_H	ρ	A_{DR}	b_{DR}	ρ	A_{DR}	b_{DR}	ρ
E1	312	1.42	0.97	155	1.39	0.98	0.52	0.26	0.71	0.50	0.25	0.88
E2	413	1.30	0.98	285	1.35	0.99	0.76	0.18	0.73	0.74	0.18	0.93
E3	432	1.44	0.98	199	1.71	0.99	0.73	0.29	0.83	0.72	0.29	0.95

Table 3: Coefficients of the relations between radar parameters (D_0, Z_H, Z_{DR}) and R and between R/Z_H and Z_{DR} for the three samples of Table 1, by considering successively 1, 2, 3 and 4 DSDs average. ρ is the correlation coefficient

		$D_0 = A_{D_0}.R^{b_{D_0}}$ $Z_H = A_{ZH}.R^{b_{ZH}}$			$Z_H = A_{ZH}.R^{b_{ZH}}$			$Z_{DR} = A_{DR}.R^{b_{DR}}$			$R/Z_H = A_{R/Z_H}.(Z_{DR})^{b_{R/Z_H}}$		
Samples	DSDs average	A_{D_0}	b_{D_0}	ρ	A_{Z_H}	b_{Z_H}	ρ	$A_{Z_{DR}}$	b_{DR}	ρ	$A_{R/Z_H}.10^3$	b_{R/Z_H}	ρ
E1	1	1.114	0.18	0.73	312	1.42	0.97	0.52	0.26	0.71	1.35	-1.45	0.95
	2	1.018	0.18	0.73	273	1.44	0.97	0.48	0.25	0.68	1.43	-1.45	0.91
	3	1.016	0.18	0.73	255	1.43	0.96	0.49	0.25	0.69	1.55	-1.45	0.91
	4	0.997	0.17	0.73	238	1.43	0.98	0.49	0.25	0.79	1.65	-1.45	0.89
E2	1	1.383	0.12	0.72	413	1.30	0.98	0.76	0.18	0.73	1.58	-1.56	0.97
	2	1.387	0.12	0.74	368	1.31	0.98	0.75	0.18	0.73	1.71	-1.62	0.95
	3	1.382	0.12	0.73	340	1.30	0.97	0.74	0.18	0.73	1.80	-1.65	0.93
	4	1.378	0.12	0.73	318	1.30	0.97	0.74	0.18	0.73	1.88	-1.69	0.91
E3	1	1.386	0.18	0.83	432	1.43	0.98	0.73	0.29	0.83	1.46	-1.50	0.97
	2	1.370	0.18	0.83	406	1.44	0.98	0.73	0.29	0.83	1.54	-1.53	0.97
	3	1.366	0.18	0.83	392	1.44	0.98	0.74	0.29	0.84	1.59	-1.55	0.96
	4	1.361	0.18	0.83	374	1.44	0.97	0.73	0.28	0.83	1.62	-1.57	0.95

less tight than for Z_H-R, this reflects the dispersion of the points in Fig. 3. They are however better with the Z_{DRt} because the recourse to (Eq. 1-3) filter the fluctuations. It noted that A_{DR} and b_{DR} are not clearly influenced by the peaks, this result suggests that the ratio Z_{DR} is not very sensitive to the shape of the distributions and the number of the drops; in fact mainly the drops of larger diameter (without influence of their number) determine Z_{DR}.

To make the discussion easier, the ratios Z_{Ht}/Z_{Hm} according to R, for each of the samples E_2 and E_3 are presented in Fig. 4. The groups of dots show clearly that the measured values are higher than the estimated values (i.e., in the absence of the peaks). The difference between the two values is all the more large as these values are high.

This difference is obviously due to the peaks which affect the shape of the measured DSD and with the effect of the large drops in the measured distributions (since these characteristics are smoothed in the theoretical DSD).

The variations of Z_{Ht}/Z_{Hm} according to R (Fig. 4) show that for R>0, 1 mm h^{-1}, this ratio increases with R. With the values of R≥2 mm h^{-1} it is constant according to R and is worth 1: the measured values are very close to the theoretical values.

Influence of the number of DSD averaged on the variance of D_0, Z_H and Z_{DR}: This study consists in examining if an integration of the real DSD at rhythms that are larger than a minute can suppress the peaks and influence the variability of the reflectivity radar.

By considering successively 1, 2, 3 and 4 DSDs average, we have, for each sample computed the relations:

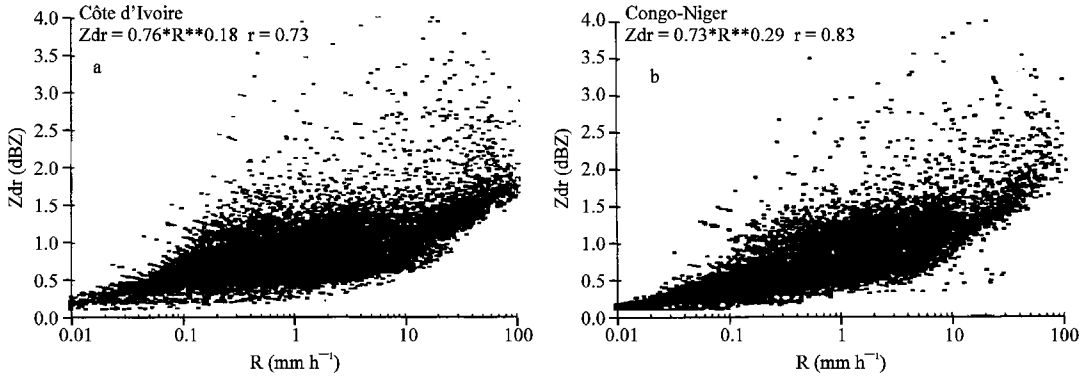

Fig. 3: Variation of Z_{Drm} as a function of R for the sample for the two sites E_2 (a) and E_3 (b)

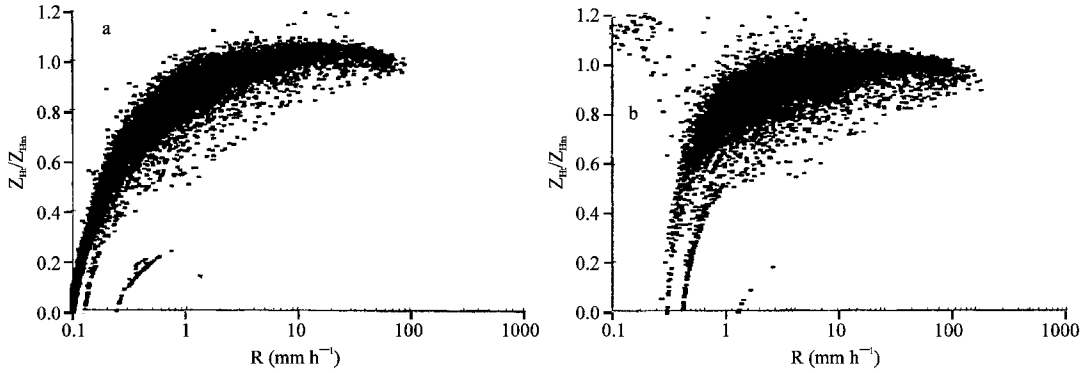

Fig. 4: Variation of the ratio Z_{Hi}/Z_{Hin} as a function of R for the sample E_2 (A) and E_3 (B)

$$D_0 = A_{D_0}.R^{b_{D_0}} \quad (R \text{ in } mm.h^{-1}, D_0 \text{ in mm}) \tag{7}$$

$$Z_{Hi} = A_{ZHi}.R^{b_{ZH}} \quad (R \text{ in } mm.h^{-1}, ZH \text{ in } mm^{-6}\ m^{-3}) \tag{8}$$

$$Z_{DR} = A_{DR}.R^{b_{DR}} \quad (R \text{ in } mm.h^{-1}, Z_{DR} \text{ in dB}) \tag{9}$$

$$R/Z_H = A_{\frac{R}{Z_H}}.(Z_{DR})^{b_{\frac{R}{Z_H}}} \quad (R \text{ in } mm.h^{-1}, ZH \text{ in } mm^6\ m^{-3} \text{ and ZDR in dB}) \tag{10}$$

Table 3 presents the coefficients of the four relations. It noted that the integration of the DSDs on 1, 2, 3 and 4 min influences slightly Eq. 7. On the other hand, Eq. 8 is largely influenced via the coefficient A_{ZH} which decreases when the average increases, whereas the coefficient b_{ZH} remains almost constant. This downward trend of the coefficient A_{ZH} approaches the result obtained with Z_H estimated by the lognormal function (Table 2). Indeed as the DSD obtained from a parameterization is deprived of peaks, one understands easily that integration (which eliminates the peaks) over several minutes of the DSD measured with the disdrometer contributes to an estimate of Z_H close to the theory. The Eq. 9-10 are subject to a slight influence of integration that is because the field of variation of Z_{DR} is very restricted. It can generally be noted, that the correlation coefficient ρ remain quasi constant with the number of integrations except for Eq. 10 where, a light reduction in ρ is noted.

Variances: Figure 5 presents the evolution of the variances $\sigma^2_{D_0}(R)$, $\sigma^2_{Z_H}(R)$ and $\sigma^2_{Z_{DR}}(R)$ for integration ranging between 1 and 4 min, for the samples of (E1) and (E3). It noted as a whole that integration slightly reduces the dispersion of Z_H, Z_{DR} and D_0 according to R. For Z_H and Z_{DR}, the values of the variance are close enough for the steps of integration (N) of 2, 3 and 4 min (min) in spite of a light reduction as N increases, that for the low values of R (R<10 mm h^{-1}). Beyond 10 mm h^{-1}, the number of integrations does not influence the variance. For D_0, the increase in the time of integration slightly improves dispersion whatever the value of R; one observes fluctuations of the variance for steps 3 and 4. It can be noted that the integration of the DSD over a few min slightly improves dispersion of the radar parameters.

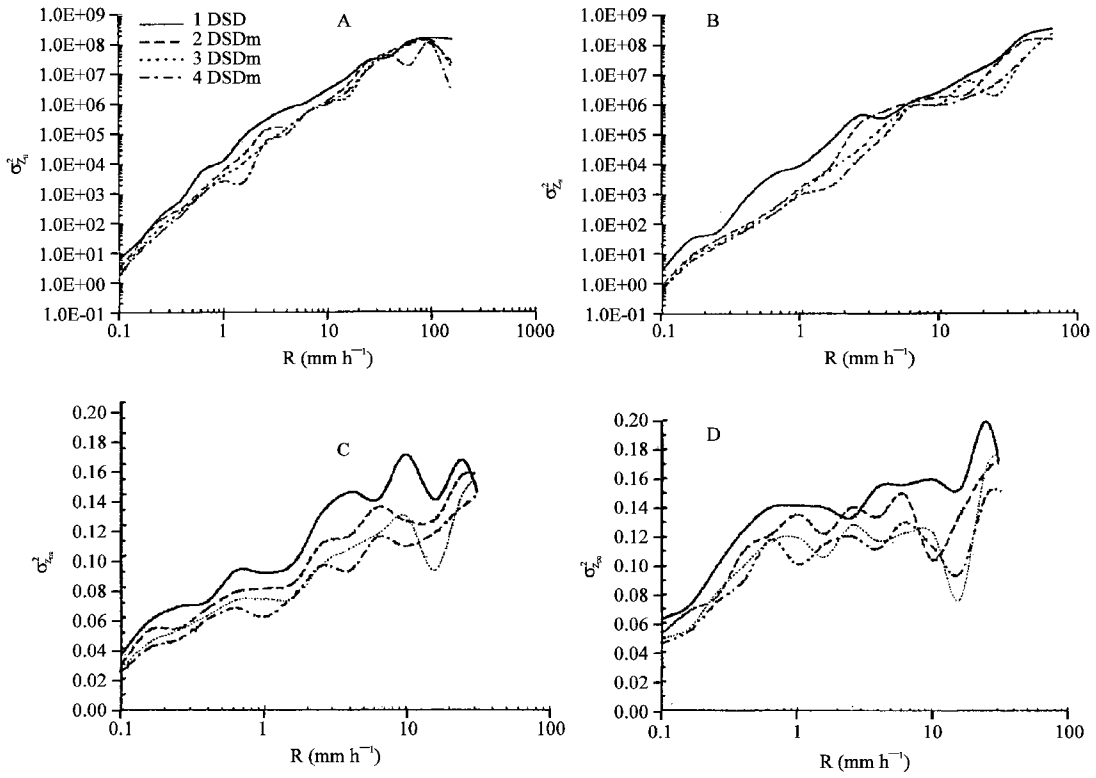

Fig. 5: Variation of $\sigma^2_{Z_H}(R)$ for the samples E_1 (A) and E_3 (B), $\sigma^2_{Z_{DR}}(R)$ for the sample E_3 (C) and $\sigma^2_{D_0}(R)$ for the sample E_3 (D)

CONCLUSIONS

The influence of the peaks on the variance of the parameters used for the precipitation measurements by polarimetric radar was the object of the study as presented in the present study. The data were the DSDs observed in tropical squall lines and in a mid-latitude frontal system.

The analysis shows a good correlation between the polarimetric parameters (Z_H and Z_{DR}) and the rain rate R. It was demonstrated that the peaks influence strongly the relation between Z_H and R, essentially the coefficients A_{ZH} but for the relation between Z_{DR} and R, they do not influence much the coefficients. The differences observed between measured values and estimated values are essentially due to the peaks. In order to explain this difference, Fig. 4 was proposed in which, the two values of Z_H are compared.

The influence of the peaks on the variability of the observable quantities by the radar was discussed. The analysis of this question as presented in this work leads to the conclusion that the relations between the integrated parameters Do, Z_{H-}, Z_{DR} and R are not very sensitive to the "width" of the step of integration used for the measurement of the DSD. When, the width of the step of integration increases, the Do-R relations are quasi unchanged, the linear coefficient of the relations Z_H-R decreases, that of the relations Z_{DR}-R is nearly constant: for the three relations, the coefficient power is unchanged. The variances of the three parameters decrease. All that shows that the influence of the peaks decreases when the step of integration increases.

ACKNOWLEDGMENTS

All the contributors to the database used in this study are gratefully acknowledged.

REFERENCES

Atlas, D. and C.W. Ulbrich, 2000. An observationally based conceptual model of warm oceanic convective rain in the tropics. J. Applied Metor., 39: 2165-2181.

Brandes, E.A., G. Zhang and J. Vivekanandan, 2002. Experiments in radar estimation with polarimetric radar in a subtropical environment. J. Applied Meteor., 41: 674-685.

Coppens, D. and Z.S. Haddad, 2000. Effects of rain drop size distribution variations on microware brightness temperature calculation. J. Geophys. Res., 105: 24483-24489.

Iguchi, T., T. Kozu, R. Meneghini, J. Awaka and K. Okamaoto, 2000. Rain-profiling algorithm for the TRMM precipitation radar. J. Applied Meteorol., 39: 2038-2052.

Ilingworth, A.J. and T.M. Blachmann, 2002. The need to represent raindrop size spectra as normalized gamma distribution for the interpretation of polarization radar observations. J. Applied Meteor., 41: 1578-1583.

Joss, J. and A. Waldvogel, 1969. Raindrop size distribution and sampling size errors. J. Atmos. Sci., 26: 566-569.

Kozu, T., K.K. Reddy, S. Mori, M. Thurai, J.T. Ong, D.N. Rao and T. Shimomai, 2006. Seasonal and diurnal variations of raindrop size distribution in Asian Monsoon Region. J. Meteorol. Soc. Jap., 84A: 195-209.

Maki, M., T.D. Keenan, Y. Sasaki and K. Nakamura, 2001. Characteristics of the raindrop size distribution in tropical continental squall lines observed in Darwin, Australia. J. Applied Meteorol., 40: 1393-1412.

McFarquhar, G.M. and R. List, 1993. The effect of curve fits for the disdrometer calibration on raindrop spectra, rainfall rate and radar reflectivity. J. Applied Meteor., 32: 774-782.

Nzeukou, A., H. Sauvageot, A.D. Ochou and C.M.F. Kebe, 2004. Rain size distribution and radar parameters at Cape Verde. J. Applied Meteorol., 43: 90-105.

Ochou, A.D., A.N. Zeukou and H. Sauvageot, 2007. Parametrization of drop size distribution with rain rate. Atmos. Res., 84: 58-66.

Sauvageot H. and J.P. Lacaux, 1995. The shape of averaged drop size distributions. J. Atmos. Sci., 52: 1070-1083.

Sauvageot, H. and M. Koffi, 2000. Multimodal raindrop size distribution. J. Atmos. Sci., 57: 2480-2492.

Seliga, T.A. and V.N. Bringi, 1976. Potential use of radar differential reflectivity measurements at orthogonal polarizations for measuring precipitation. J. Applied Meteor., 15: 69-76.

Sheppard, B.E., 1990. Effect of irregularities in the diameter classification of raindrop by the Joss-Waldvogel disdrometer. J. Atmos. Oceanic Technol., 7: 180-183.

Testud, J., S. Oury, R.A. Black, P. Amayene and X. Dou, 2001. The concept of normalized distribution to describe raindropsoectra. A tool for cloud physics and cloud remote sensing. J. Applied Meteor., 40: 1118-1140.

Tokay, A., A. Kruger and W.F. Krajewski, 2001. Comparison of drop size distribution measurements by impact and optical disdrometers. J. Applied Meteorol., 40: 2083-2097.

Uijlenhoet, R., M. Steiner and J.A. Smith, 2003. Variability of raindrop size distribution in a squall line and implication for radar rainfall estimation. J. Hydrometeor., 4: 43-61.